Inorg. Chem. **2006**, *45*, 9890–9900

Spacially Confined M_2 Centers (M = Fe, Co, Ni, Zn) on a Sterically Bulky Binucleating Support: Synthesis, Structures and Ethylene Oligomerization Studies

Yohan D. M. Champouret, John Fawcett, William J. Nodes, Kuldip Singh, and Gregory A. Solan*

Department of Chemistry, University of Leicester, University Road, Leicester LE1 7RH, U.K.

Received July 12, 2006

Two new bulky aryl-bridged pyridyl-imine compartmental (pro)ligands, 2,6-{(2,6-*i*-$Pr_2C_6H_3$)N═C(Me)C_5H_3N}$_2C_6H_3$Y (Y = H **L**^{1}, OH **L**^{2}-H), have been prepared in moderate to good overall yields via a Stille-type cross-coupling approach. The molecular structure of **L**^{2}-H reveals a transoid configuration within the pyridyl-imine units with a hydrogen-bonding interaction maintaining the phenol coplanar with one of the adjacent pyridine rings. The interaction of 2 equiv of MX_2 with **L**^{1} in *n*-BuOH at 110 °C gives the binuclear complexes, [(**L**^{1})M_2X_4] (M = Fe, X = Cl (**1a**); M = Co, X = Cl (**1b**); M = Ni, X = Br (**1c**); M = Zn, X = Cl (**1d**)), in which the metal centers adopt distorted tetrahedral geometries and occupy the two pyridyl-imine cavities in **L**^{1}. In contrast, deprotonation of **L**^{2}-H occurs upon reaction with 2 equiv of MX_2 to afford the phenolate-bridged species [(**L**^{2})$M_2(\mu$-X)X_2] (M = Fe, X = Cl (**2a**); M = Co, X = Cl (**2b**); M = Ni, X = Br (**2c**); M = Zn, X = Cl (**2d**)). ^{1}H NMR studies of diamagnetic **1d** and **2d** reveal that the limited rotation of the *N*-aryl groups in **1d** is further impeded in **2d** by steric interactions imparted by the two closely located *N*-aryl groups. Partial displacement of the bridging bromide in **2c** results upon its treatment with acetonitrile to afford [(**L**^{2})Ni_2Br_3(NCMe)] [**2c**(MeCN)]; no such reaction occurs for **2a**, **2b**, or **2d**. Upon activation with excess methylalumoxane (MAO), **1b**, **1c**, **2b**, and **2c** show some activity for alkene oligomerization forming low molecular-weight materials with methyl-branched products predominating for the nickel systems. Single-crystal X-ray diffraction studies have been performed on **L**^{2}-H, **1c**, **2b**, **2c**, **2c**(NCMe), and **2d**.

Introduction

The use of binucleating ligands as a means to impose close spacial confinement on two metal centers has been widely documented due, in part, because of the relevance of the resulting bimetallic complexes to the active sites of a variety of naturally occurring metalloenzymes.[1] Moreover, the potential for unique reactivity patterns and unusual catalytic properties exhibited by synthetic examples of such dinuclear species has further fueled research activity in the field.[2] With regard to polymerization applications, encapsulated two-center systems have started to be employed as catalysts for a range of metal-mediated processes including ring-opening[3] and alkene polymerization.[4−8] Indeed, good catalytic performances have been observed, and cooperative effects by the neighboring polymerization-active metal centers have been suggested.

Within the alkene polymerization/oligomerization arena, the use of compartmentalized LM_2 systems incorporating early transition metals has been at the heart of many of the key developments,[4,5] while the use of late transition metal

* To whom the correspondence should be addressed. E-mail: gas8@leicester.ac.uk.

(1) For reviews, see: (a) Gavrilova, A. L.; Bosnich, B. *Chem. Rev.* **2004**, *104*, 349. (b) van den Beuken, E. K.; Feringa, B. L. *Tetrahedron* **1998**, *54*, 12985. (c) Steinhagen, H.; Helmchen, G. *Angew. Chem., Int. Ed. Engl.* **1996**, *35*, 2339. (d) Sträter, N.; Lipscomb, W. N.; Klaubunde, T.; Krebs, B. *Angew. Chem., Int. Ed. Engl.* **1996**, *35*, 2024. (e) Belle, C.; Pierre, J.-L. *Eur. J. Inorg. Chem.* **2003**, 4137. (f) Fenton, F. E. *Chem. Soc. Rev.* **1999**, *28*, 159.

(2) (a) Saied, O.; Simard, M.; Wuest, J. D. *Organometallics* **1996**, *15*, 2345. (b) Ooi, T.; Takahashi, M.; Yamada, M.; Tayama, E.; Omoto, K.; Maruoka, K. *J. Am. Chem. Soc.* **2004**, *126*, 1150. (c) Kumagai, N.; Matsunaga, S.; Kinoshita, T.; Harada, S.; Okada, S.; Sakamoto, S.; Yamaguchi, K.; Shibasaki, M. *J. Am. Chem. Soc.* **2003**, *125*, 2169. (d) Trost, B. M.; Silcoff, E. R.; Ito, H. *Org. Lett.* **2001**, *3*, 2497. (e) Trost, B. M.; Yeh, V. S. C.; Ito, H.; Bremeyer, N. *Org. Lett.* **2002**, *4*, 2621. (f) Trost, B. M.; Ito, H.; Silcoff, E. R. *J. Am. Chem. Soc.* **2001**, *123*, 3367. (g) Trost, B. M.; Fettes, A.; Shireman, B. T. *J. Am. Chem. Soc.* **2004**, *126*, 2660. (h) Gao, J.; Reibenspies, J. H.; Martell, A. E. *Angew. Chem., Int. Ed.* **2993**, *42*, 6008.

(3) (a) Breyfigle, L. E.; Williams, C. K.; Young, V. G., Jr.; Hillmyer, M. A.; Tolman, W. *Dalton Trans.* **2006**, 928. (b) Lee, B. Y.; Kwon, H. Y.; Lee, S. Y.; Na, S. J.; Han, S.-i; Yun, H.; Lee, H.; Park, Y.-W. *J. Am. Chem. Soc.* **2005**, *127*, 3031. (c) Williams, C. K.; Brooks, N. R.; Hillmyer, M. A.; Tolman, W. B. *Chem. Commun.* **2002**, 2132.

10.1021/ic061286x CCC: $33.50
Published on Web 10/24/2006

combinations has only recently started to emerge in the literature.[6−8] By appreciation of the important role played by steric bulk in late transition metal-mediated polymerizations,[9] a range of sterically encumbered multidentate binucleating ligands (e.g., organo-bridged iminopyridines, α-diimines, and iminophenolates) have been found to be compatible supports for active dinickel,[6a,7] dipalladium,[8] and diiron catalysts.[6] However to date, because of the nature of the binucleating ligand design, the late metal centers tend to be positioned at the extremities of the ligand manifold and thus would be expected to limit potential cooperative metal−metal interactions.

With the intent of forcing the late metal centers into closer proximity, we have targeted the novel sterically demanding neutral bis(iminopyridyl)benzene (**L**^{1}) and monoanionic bis(iminopyridyl)phenolate [(**L**^{2})$^-$] ligands as potential supports for homobimetallic iron(II), cobalt(II), nickel(II), and zinc(II) complexes (Figure 1). Herein, we report full details of ligand synthesis along with the resultant coordination chemistry. In addition, selected examples of the complexes are screened as precatalysts for ethylene oligomerization.

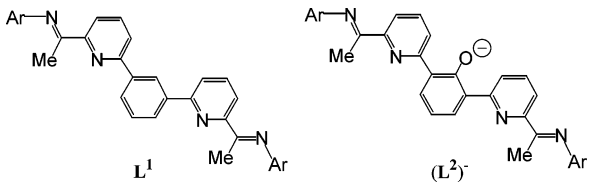

Figure 1. Bis(iminopyridyl)benzene (**L**^{1}) and bis(iminopyridyl)phenolate [(**L**^{2})$^-$]; Ar = 2,6-*i*-$Pr_2C_6H_3$.

Results and Discussion

Ligand synthesis. Treatment of 2,6-{O=C(Me)-C_5H_3N}$_2C_6H_3Y$ (Y = H, OH) with 2,6-diisopropylaniline, as both reactant and solvent, at elevated temperature in the presence of a catalytic amount of formic acid produced 2,6-{(2,6-*i*-$Pr_2C_6H_3$)N=C(Me)C_5H_3N}$_2C_6H_3Y$ (Y = H (**L**^{1}), OH (**L**^{2}-H)) in moderate yield (Scheme 1). The diketones, 2,6-{O=C(Me)C_5H_3N}$_2C_6H_3Y$ (Y = H, OH), have not been previously reported and could be prepared in moderate to good overall yield in two steps by treating first 1,3-dibromobenzene or 2,6-dibromophenol with 2-(*n*-BuSn)-6-{C(Me)CH_2CH_2O}-C_5H_3N[10] under standard Stille cross-coupling conditions,[11] followed by acid deprotection. In the case of 2,6-{O=C(Me)C_5H_3N}$_2C_6H_3OH$, the formation of the homo-coupled product, 6,6″-diacetyl-2,2′:6′,2″-bipyridine,[12] proved to be a competitive reaction pathway which could be significantly inhibited by the addition of catalytic amounts of cuprous bromide to the Stille reaction (see Experimental Section).[13] All the new compounds have been characterized by ^{1}H NMR, ^{13}C NMR, and IR spectroscopy, electrospray (ES) mass spectrometry, or elemental analysis. In addition, a crystal of **L**^{2}-H has been the subject of a single-crystal X-ray diffraction study.

The molecular structure of **L**^{2}-H is depicted in Figure 2; selected bond lengths and angles are listed in Table 1. Crystals suitable for the X-ray structure determination were grown by slow evaporation of a chloroform solution containing the compound. The molecular structure of **L**^{2}-H consists of a central phenol group linked at its 2 and 6 positions by two pyridyl-imine units. Within each unit, the pyridyl and imine moieties are almost coplanar [N(1)−C(13)−C(15)−N(2) = 3.2° and N(3)−C(30)−C(31)−N(4) = 2.4°] with the respective nitrogen atoms disposed mutually trans. The hydroxy proton of the central phenol group undergoes a hydrogen-bonding interaction [O(1)···N(2) = 2.557(2) Å] with one of the neighboring pyridine nitrogen atoms [N(2)] resulting in one of the pyridyl-imine units being almost coplanar with the central phenol plane [C(25)−C(20)−C(19)−N(2) = 3.7°], while the other is inclined at 18.6°. The 2,6-diisopropylphenyl substituents on each imino group

(4) (a) Li, H.; Stern C. L.; Marks, T. J. *Macromolecules* **2005**, *38*, 9015. (b) Li, H.; Li, L.; Schwartz, D. J.; Metz, M. V.; Marks, T. J.; Liable-Sands L.; Rheingold, A. L. *J. Am. Chem. Soc.* **2005**, *127*, 14756. (c) Guo, N.; Li, L.; Marks, T. J. *J. Am. Chem. Soc.* **2004**, *126*, 6542. (c) Noh, S. K.; Lee, M.; Kum, D. H.; Kim, K.; Lyoo, W. S.; Lee, D.-H. *J. Polym. Sci., Part A: Polym. Chem.* **2004**, *42*, 1712.

(5) (a) Liu, X.; Sun, J.; Zhang, H.; Xiao, X.; Lin, F. *Eur. Polym. J.* **2005**, *41*, 1519. (b) Juengling, S.; Mülhaupt, R.; Plenio, H. *J. Organomet. Chem.* **1993**, *460*, 191. (c) Yan, X.; Chernega, A.; Green, M. L. H.; Sanders, J.; Souter, J.; Ushioda, T. *J. Mol. Catal. A: Chem.* **1998**, *128*, 119. (d) Desurmont, G.; Li, Y.; Yasuda, H.; Maruo, T.; Kanehisa, N.; Kai, Y. *Organometallics* **2000**, *19*, 1811. (e) Noh, S. K.; Kim, J.; Jung, J.; Ra, C. S.; Lee, D.-H.; Lee, H. B.; Lee, S. W.; Huh, W. S. *J. Organomet. Chem.* **1999**, *580*, 90. (f) Diamond, G. M.; Chernega, A. N.; Mountford, P.; Green, M. L. H. *J. Chem. Soc., Dalton Trans.* **1996**, 921. (g) Larkin, S. A.; Golden, J. T.; Shapiro, P. J.; Yap, G. P. A.; Foo, D. M. J.; Rheingold, A. L. *Organometallics* **1996**, *15*, 2393. (h) Green, M. L. H.; Popham, N. H. *J. Chem. Soc., Dalton Trans.* **1999**, 1049. (i) Huang, J.; Feng, Z.; Wang, H.; Qian, Y.; Sun, J.; Xu, Y.; Chen, W.; Zheng, G. *J. Mol. Catal. A: Chem.* **2002**, *189*, 187. (j) Ushioda, T.; Green, M. L. H.; Haggitt, J.; Yan, X. *J. Organomet. Chem.* **1996**, *518*, 155. (k) Jung, J.; Noh, S. K.; Lee, D.-H.; Park, S. K.; Kim, K. *J. Organomet. Chem.* **2000**, *595*, 147. (l) Noh, S. K.; Kim, S.; Kim, J.; Lee, D.-H.; Yoon, K.-B.; Lee, H.-B.; Lee, S. W.; Huh, W. S. *J. Polym. Sci., Part A: Polym. Chem.* **1997**, *35*, 3717. (m) Mitani, M.; Oouchi, K.; Hayakawa, M.; Yamada, T.; Mukaiyama, T. *Polym. Bull. (Berlin)* **1995**, *35*, 677.

(6) Solan, G. A.; Pelletier, J. D. A. (ExxonMobil Chemical Patents, Inc.) International Patent WO 2005118605, 2005. (b) Small, B. L. (Chevron Phillips Chemical Company), U.S. Patent 2004180778, 2004.

(7) (a) Hu, T.; Tang, L.-M.; Li, X.-F.; Li, Y.-S.; Hu, N.-H. *Organometallics* **2005**, *24*, 2628. (b) Zhang D.; Jin, G.-X. *Organometallics* **2003**, *22*, 2851. (c) Luo, H.-K.; Schumann, H. *J. Mol. Catal. A: Chem.* **2005**, *227*, 153. (d) Jie, S.; Zhang, D.; Zhang, T.; Sun, W.-H.; Chen, J.; Ren, Q.; Liu, D.; Zheng, G.; Chen., W. *J. Organomet. Chem.* **2005**, *690*, 1739. (e) Mi, X.; Ma, Z.; Wang, L.; Ke, Y.; Hu, Y. *Macromol. Chem. Phys.* **2003**, *204*, 868. (f) Gibson, V. C.; Halliwell, C. M.; Long, N. J.; Oxford, P. J.; Smith, A. M.; White A. J. P.; Williams, D. J. *Dalton Trans.* **2003**, 918. (g) Tomov, A. Kurtev, K. *J. Mol. Catal. A: Chem.* **1995**, *103*, 95. (h) Kurtev, K.; Tomov, A. *J. Mol. Catal.* **1994**, *88*, 141. (i) Taquet, J.-P.; Siri, O.; Braunstein, P.; Welter, R. *Inorg. Chem.* **2006**, *45*, 4668.

(8) (a) Chen, R.; Bacsa, J.; Mapolie, S. F. *Polyhedron* **2003**, *22*, 2855. (b) Chen, R.; Mapolie, S. F. *J. Mol. Catal. A: Chem.* **2003**, *193*, 33. (c) Bianchini, C.; Gonsalvi, L.; Oberhauser, W.; Semeril, D.; Brueggeller, P.; Gutmann, R. *Dalton Trans.* **2003**, 3869.

(9) (a) Gibson, V. C.; Wass, D. F. *Angew. Chem., Int. Ed. Engl.* **1999**, *38*, 419. (b) Gibson, V. C.; Spitzmesser, S. *Chem. Rev.* **2003**, *103*, 283. (c) Ittel, S. D.; Johnson, L. K.; Brookhart, M. *Chem. Rev.* **2000**, *100*, 1169. (d) Mecking, S. *Angew. Chem., Int. Ed.* **2001**, *40*, 534.

(10) Champouret, Y. D. M.; Chaggar, R. K.; Dadhiwala, I.; Fawcett, J.; Solan, G. A. *Tetrahedron* **2006**, *62*, 79.

(11) (a) Stille, J. K. *Angew. Chem., Int. Ed. Engl.* **1986**, *25*, 508. (b) Espinet, P.; Echavarren, A. M. *Angew. Chem., Int. Ed.* **2004**, *43*, 4707.

(12) (a) Jones, G.; Pitman, M. A.; Lunt, E.; Lythgoe, D. J.; Abarca, B. *Tetrahedron* **1997**, *53*, 8257. (b) Parks, J. E.; Wagner, B. E.; Holm, R. H. *J. Organomet. Chem.* **1973**, *56*, 53. (c) Potts, K. T.; Raiford, K. A. G.; Keshavarz-K, M. *J. Am. Chem. Soc.* **1993**, *115*, 2793.

(13) (a) Liebeskind, L. S.; Fengl, R. W. *J. Org. Chem.* **1990**, *55*, 5359. (b) Farina, V. *Pure Appl. Chem.* **1996**, *68*, 73. (c) Wang, Y.; Burton, D. J. *Org. Lett.* **2006**, *8*, 1109. (d) Farina, V.; Kapadia, S.; Krishnan, B.; Wang, C.; Liebeskind, L. S. *J. Org. Chem.* **1994**, *59*, 9, 5905.

Scheme 1 [a]

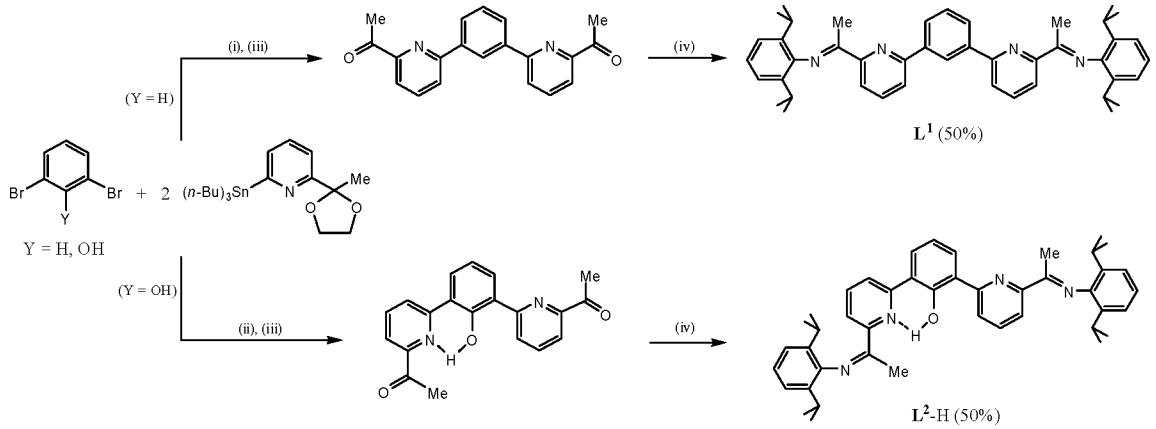

[a] Reagents and conditions: (i) $Pd(PPh_3)_4$ (16 mol %), toluene, 90 °C, 72 h; (ii) $Pd(PPh_3)_4$ (8 mol %), CuBr (16 mol %), toluene, 100 °C, 72 h; (iii) HCl (4 M), 60 °C, 12 h; (iv) 2,6-*i*-$Pr_2C_6H_3NH_2$, 160 °C, cat. H^+.

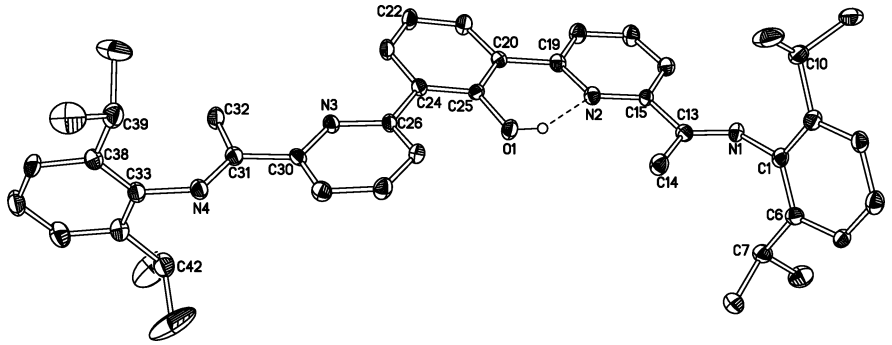

Figure 2. Molecular structure of $\mathbf{L^2}$-H with atom labeling scheme and ellipsoids at 30% probability. All hydrogen atoms, apart from H1, have been omitted for clarity.

Table 1. Selected Bond Distances (Å) and Angles (deg) for $\mathbf{L^2}$-H

N(1)−C(13)	1.281(4)	O(1)−C(25)	1.354(4)
N(4)−C(31)	1.277(4)	C(24)−C(26)	1.501(4)
C(13)−C(14)	1.491(4)	C(19)−C(20)	1.492(4)
C(31)−C(32)	1.506(4)	C(13)−C(15)	1.492(4)
C(13)−N(1)−C(1)	121.0(3)	C(15)−N(2)−C(19)	119.8(3)
C(30)−N(3)−C(26)	119.1(3)	C(31)−N(4)−C(33)	120.6(3)

are oriented almost orthogonally to their adjacent pyridylimine planes [C(13)−N(1)−C(1)−C(6) = 87.4°, C(31)−N(4)−C(33)−C(34) = 84.5°]. The magnitude of the imino C−N bond lengths [C(13)−N(1) = 1.281(4) Å, C(31)−N(4) = 1.277(4) Å] is consistent with the presence of double-bond character.

In the solution state, however, the solid-state properties of $\mathbf{L^2}$-H are not maintained, and the molecule possesses a C_2 plane of symmetry about the O(1)−C(25)−C(22) axis. Similarly in $\mathbf{L^1}$, the ^{1}H NMR spectrum reveals each pyridylimine unit to be equivalent. In addition, characteristic signals at ∼166 ppm are seen for the *C*═N carbon atoms in their ^{13}C NMR spectra, while the *Me*C═N protons are seen as singlets at ∼2.3 ppm in their ^{1}H NMR spectra. It is noteworthy that for both $\mathbf{L^1}$ and $\mathbf{L^2}$-H some restricted rotation of the isopropyl groups is apparent with two closely located sets of doublets for the CH*Me*$_2$ groups evident in their ^{1}H NMR spectra. The ES mass spectra of $\mathbf{L^1}$ and $\mathbf{L^2}$-H show peaks corresponding to the protonated molecular ion for each ligand. In the IR spectra of $\mathbf{L^1}$ and $\mathbf{L^2}$-H, characteristic absorption bands for ν(C═N) stretches are seen at ∼1639 cm^{-1}.

Synthesis of Complexes. The reaction of $\mathbf{L^1}$ with 2 equiv of MX_2 [MX_2 = $FeCl_2$, $CoCl_2$, (DME)$NiBr_2$, $ZnCl_2$] in *n*-butanol at elevated temperatures gave complexes [($\mathbf{L^1}$)M_2X_4] (M = Fe, X = Cl (**1a**); M = Co, X = Cl (**1b**); M = Ni, X = Br (**1c**); M = Zn, X = Cl (**1d**)) in moderate yields (Scheme 2). Similarly, complexes [($\mathbf{L^2}$)M_2(μ-X)X_2] (M = Fe, X = Cl (**2a**); M = Co, X = Cl (**2b**); M = Ni, X = Br (**2c**); M = Zn, X = Cl (**2d**)) were prepared in good yield by treating 2 equiv of MX_2 [MX_2 = $FeCl_2$, $CoCl_2$, (DME)$NiBr_2$, $ZnCl_2$] with proligand $\mathbf{L^2}$-H in *n*-butanol at elevated temperature (Scheme 2); no additional base was needed in any of the transformations. All products have been characterized by FAB mass spectrometry, IR spectroscopy, and in the cases of **1a**−**1c** and **2a**−**2c**, by magnetic measurements, while diamagnetic **1d** and **2d** were characterized by ^{1}H NMR spectroscopy (see Table 2 and Experimental Section). In addition, **1c** and **2b**−**2d** have been the subject of single-crystal X-ray diffraction studies.

Crystals of **1c** suitable for the X-ray determination were grown by slow cooling of a hot acetonitrile solution containing the complex. A view of **1c** is depicted in Figure 3; selected bond distances and angles are listed in Table 3. The molecular structure of **1c** reveals a bimetallic complex in which the two metal centers are supported on the same $\mathbf{L^1}$ ligand frame and each bound terminally by two bromide

Scheme 2 [a]

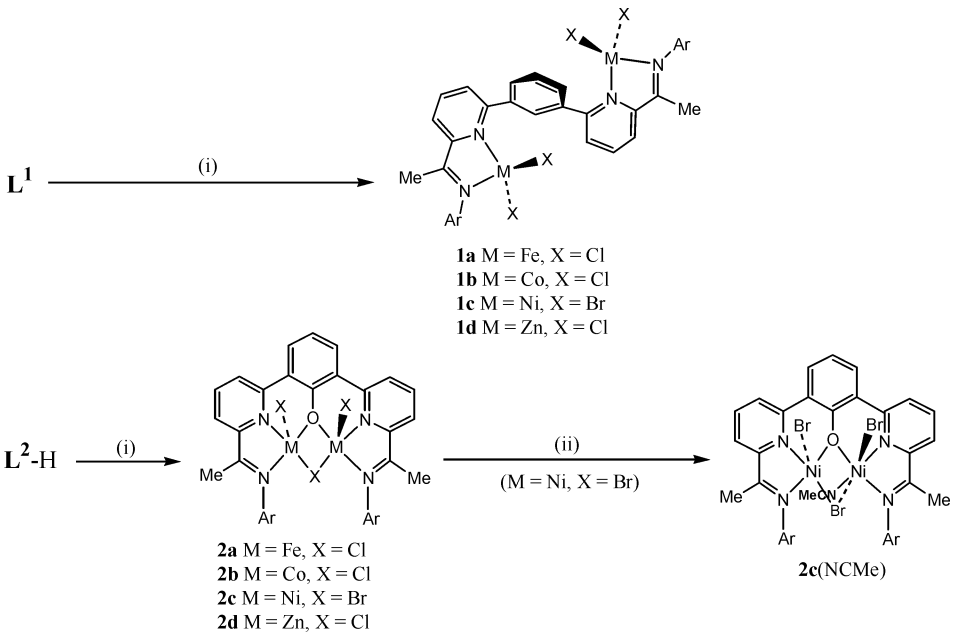

[a] Reagents and conditions: (i) 2 MX_2 [MX_2 = $FeCl_2$, $CoCl_2$, (DME)$NiBr_2$, $ZnCl_2$], *n*-butanol, 110 °C; (ii) MeCN, heat (Ar = 2,6-*i*-$Pr_2C_6H_3$).

Table 2. Selected Characterization Data for the New Complexes **1** and **2**

complex	color	ν(C=N) (cm^{-1})[a]	μ_{eff} (μ_B)[b]	FAB mass spectrum	microanalysis (%)[c] C	H	N
1a	brown	1593	7.4	888 $[M]^+$, 852 $[M - Cl]^+$			
1b	blue	1593	5.1	858 $[M - Cl]^+$, 823 $[M - 2Cl]^+$	58.98 (59.07)	5.51 (5.63)	6.13 (6.26)
1c	red	1594	4.3	991 $[M]^+$, 912 $[M - Br]^+$	49.51 (49.30)	4.71 (4.70)	5.17 (5.23)
1d	yellow	1592	*d*	871 $[M - Cl]^+$, 836 $[M - 2Cl]^+$	58.05 (58.23)	5.55 (5.55)	6.11 (6.17)
2a	brown	1588	5.7	866 $[M]^+$, 831 $[M - Cl]^+$	53.38 (53.40)[e]	5.24 (4.94)[e]	5.26 (5.51)[e]
2b	blue-green	1586	4.7	837 $[M - Cl]^+$	60.52 (60.46)	5.59 (5.65)	6.41 (6.41)
2c	red	1589	3.4	927 $[M - Br]^+$, 846 $[M - 2Br]^+$	48.83 (49.00)[e]	4.63 (4.54)[e]	5.09 (5.11)[e]
2c(NCMe)	red	1588 $2300_{\nu(C\equiv N)}$	3.5	927 $[M - Br - NCMe]^+$, 846 $[M - 2Br - NCMe]^+$	50.65 (50.85)[e]	4.44 (4.75)[e]	5.25 (5.35)[e]
2d	yellow	1589	*d*	851 $[M - Cl]^+$	59.44 (59.58)	5.59 (5.51)	6.25 (6.17)

[a] Recorded on a Perkin-Elmer Spectrum One FT-IR spectrometer on solid samples. [b] Recorded on an Evans Balance at room temperature. [c] Calculated values shown in parentheses. [d] Sample diamagnetic. [e] Calculated values include *x*$CHCl_3$ [where *x* = 1.25 (**2a**), 0.75 (**2c**), 0.5 [**2c**(NCMe)]].

ligands. The geometry at each nickel center can be best described as distorted tetrahedral with the $N_{imine}-Ni-N_{pyridine}$ bite angle similar in size at both pyridyl-imine cavities [N(1)−Ni(1)−N(2) = 81.03(17)° vs N(3)−Ni(2)−N(4) = 82.95(16)°] but with significantly different Br−Ni−Br bond angles [Br(1)−Ni(1)−Br(2) = 109.02(3)° vs Br(3)−Ni(2)−Br(4) = 125.22(4)°]. Both imino-pyridyl moieties are quasi-planar [N(1)−C(7)−C(9)−N(2) = 2.2°, N(3)−C(24)−C(25)−N(4) = 3.1°] and are oriented essentially orthogonally to the *N*-aryl groups [C(2)−C(1)−N(1)−C(7) = 94.0°, C(28)−C(27)−N(4)−C(25) = 90.2°]. In addition, the central aryl group is tilted away from coplanarity with respect to both adjacent pyridyl-imine units [N(3)−C(20)−C(18)−C(19) = 47.8°, C(19)−C(14)−C(13)−N(2) = 42.9°]. The Ni−Br bond lengths at each metal center are inequivalent with the discrepancy most noticeable at Ni(1) with a difference of 0.04 Å apparent. The Ni−N distances are similar and compare well with other crystallographically characterized pyridyl-imine-$NiBr_2$-containing complexes.[7d,14] The imino carbon−nitrogen bond lengths [C(7)−N(1) = 1.290(6) Å, C(25)−N(4) = 1.279(6) Å] are essentially equivalent and consistent with double-bond character. An inspection of the intermetallic distance [5.223(4) Å] reveals that there is no direct Ni···Ni interaction between the two metal centers.

(14) (a) Laine, T. V.; Klinga, M.; Leskela, M. *Eur. J. Inorg. Chem.* **1999**, 959. (b) Laine, T. V.; Piironen, U.; Lappalainen, K.; Klinga, M.; Aitola, E.; Leskela, M. *J. Organomet. Chem.* **2000**, *606*, 112. (c) Tang, X.; Sun, W.-H.; Gao, T.; Hou, J.; Chen, J.; Chen, W. *J. Organomet. Chem.* **2005**, *690*, 1570. (d) Britovsek, G. J. P.; Baugh, S. P. D.; Hoarau, O.; Gibson, V. C.; Wass, D. F.; White, A. J. P.; Williams, D. J. *Inorg. Chim. Acta* **2003**, *345*, 279. (e) Nienkemper, K.; Kotov, V. V.; Kehr, G.; Erker, G.; Fröhlich, R. *Eur. J. Inorg. Chem.* **2006**, 366.

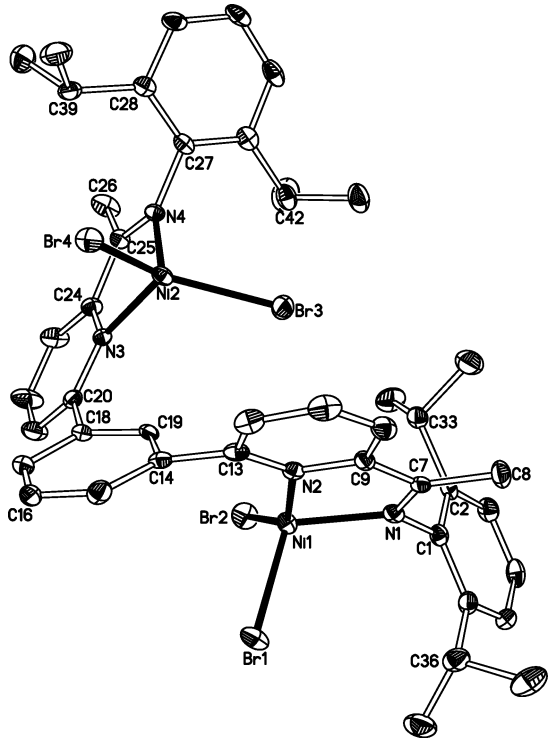

Figure 3. Molecular structure of **1c** with atom labeling scheme and ellipsoids at 30% probability. All hydrogen atoms have been omitted for clarity.

Table 3. Selected Bond Distances (Å) and Angles (deg) for **1c**

Ni(1)−N(1)	2.006(4)	Ni(1)−Br(1)	2.3742(9)
Ni(1)−N(2)	2.023(4)	Ni(1)−Br(2)	2.3296(9)
Ni(2)−N(3)	2.003(4)	Ni(2)−Br(3)	2.3511(10)
Ni(2)−N(4)	2.022(4)	Ni(2)−Br(4)	2.3475(9)
C(7)−N(1)	1.290(6)	C(25)−N(4)	1.279(6)
Ni(1)···Ni(2)	5.223(4)		
N(1)−Ni(1)−N(2)	81.03(17)	N(3)−Ni(2)−N(4)	82.95(16)
Br(1)−Ni(1)−N(1)	107.64(11)	Br(3) Ni(2)−N(3)	115.90(12)
Br(2)−Ni(1)−N(1)	114.27(12)	Br(4)−Ni(2)−N(3)	105.88(12)
Br(1)−Ni(1)−N(2)	94.79(11)	Br(3) Ni(2)−N(4)	105.10(12)
Br(2)−Ni(1)−N(2)	144.64(12)	Br(4)−Ni(2)−N(4)	114.00(12)
Br(1)−Ni(1)−Br(2)	109.02(3)	Br(3)−Ni(2)−Br(4)	125.22(4)

The FAB mass spectra for **1a**−**1d** show fragmentation peaks corresponding to the loss of one or two halide groups from the corresponding molecular ion peak of each complex. In their IR spectra, the ν(C═N)$_{imine}$ bands are seen at ∼1592 cm^{-1} and are shifted to a lower wavenumber by ∼49 cm^{-1} in comparison with free $\mathbf{L^1}$; an observation that is in accordance with the nitrogen atoms of the imino groups [N(1), N(4)] being bound. Complexes **1a**−**1c** are all paramagnetic displaying magnetic moments of 7.2, 5.1, and 4.3 μ_B (Evans Balance at ambient temperature), their values being consistent with two noninteracting high-spin Fe(II)−Fe(II) (S = 2 and 2, respectively), Co(II)−Co(II) (S = 3/2 and 3/2, respectively), and Ni(II)−Ni(II) (S = 1 and 1, respectively) metal centers, respectively (using $\mu^2 = \sum\mu_i^2$, where μ_i is the magnetic moment of the individual metal centers).[15] In contrast, complex **1d** is diamagnetic and shows a ^{1}H NMR spectrum (in $CDCl_3$ at ambient temperature) that supports molecular C_2 symmetry in solution with the equivalent imino-methyl signals (at 2.40 ppm) being shifted downfield by 0.14 ppm upon coordination. Notably, the solution behavior of **1d** can be compared to [{2,6-{(2,6-*i*-Pr$_2$C$_6$H$_3$)N═C(Me)C$_5$H$_3$N}$_2$C$_5$H$_3$N}Zn$_2$Cl$_4$] in which disconnection of the central pyridine group was invoked to account for the observed C_2 symmetry.[16] As with the free ligand $\mathbf{L^1}$, restricted rotation of the aryl groups in **1d** leads to two sets of doublets for the CH(CH_3)$_2$ groups in the ^{1}H NMR spectrum; the separation between signals is, however, more pronounced for **1d**.

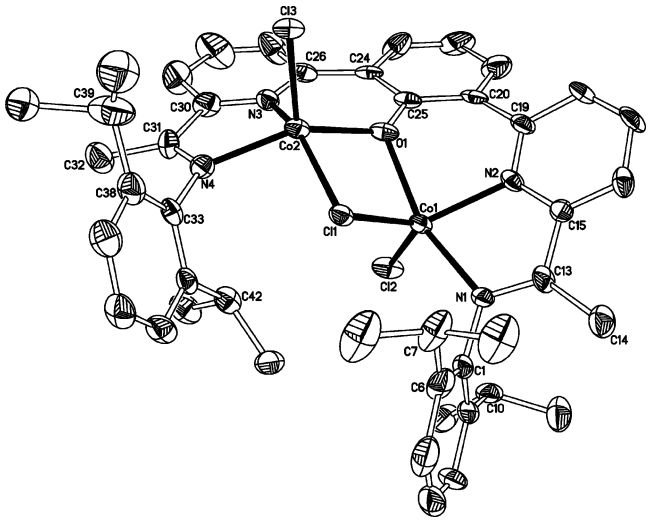

Figure 4. Molecular structure of **2b** with atom labeling scheme and ellipsoids at 30% probability. All hydrogen atoms have been omitted for clarity.

Single crystals of **2** suitable for the X-ray determination were grown from mixtures of acetonitrile−chloroform (**2b** and **2d**) and chloroform−diethyether (**2c**). A view of **2b** is depicted in Figure 4; selected bond distances and angles are listed for all three species in Table 4. The structures of **2b**−**2d** are similar and will be discussed together. The molecular structures comprise two metal atoms supported on the same monoanionic $(\mathbf{L^2})^-$ ligand frame with the phenolate oxygen atom [O(1)] bridging the metals and the two separate pyridyl-imine units acting as chelates. Each metal center is further bound by one terminal halide and one bridging halide to complete two independent five-coordinate geometries. Some differences in the coordination sphere at each metal center are observed with the geometry at M(1) being best described as distorted square pyramidal [τ = 0.51 at Co(1) (**2b**), 0.50 at Ni(1) (**2c**), and 0.38 at Zn(1) (**2d**)],[17] while at M(2), a more idealized square pyramidal geometry is evident [τ = 0.06 at Co(2) (**2b**), 0.02 Ni(2) (**2c**), and 0.07 at Zn(2) (**2d**)]. The imino-pyridyl chelating moieties in $(\mathbf{L^2})^-$ are almost planar [N(1)−C(13)−C(15)−N(2) = 4.9 (**2b**), 14.0 (**2c**), and 7.1° (**2d**); N(3)−C(30)−C(31)−N(4) = 7.7 (**2b**), 5.0 (**2c**), and 10.0° (**2d**)] with the *N*-aryl groups almost orthogonal to these planes [C(2)−C(1)−N(1)−C(13) = 90.1 (**2b**), 91.3 (**2c**), and 93.3° (**2d**); C(34)−C(33)−N(4)−C(31) = 100.4 (**2b**), 92.1 (**2c**), and 99.1° (**2d**)]. These inclinations of the

(15) Gerli, A.; Hagen, K. S.; Marzilli, L. G. *Inorg. Chem.* **1991**, *30*, 4673.

(16) Champouret, Y. D. M.; Maréchal, J.-D.; Dadhiwala, I.; Fawcett, J.; Palmer, D.; Singh, K.; Solan, G. A. *Dalton Trans.* **2006**, 2350.

(17) For use of τ, see: Addison A. W.; Rao, T. N.; Reedijk, J.; von Rijn J.; Verschoor, G. C. *J. Chem. Soc., Dalton Trans.* **1984**, 1349.

Table 4. Selected Bond Distances (Å) and Angles (deg) for **2b**, **2c**, and **2d**

	M = Co, X = Cl (**2b**)	M = Ni, X = Br (**2b**)	M = Zn, X = Cl (**2d**)
M(1)−N(2)	2.070(6)	2.010(5)	2.077(4)
M(1)−O(1)	2.096(5)	2.012(4)	2.141(3)
M(1)−N(1)	2.149(6)	2.087(4)	2.178(4)
M(1)−X(2)	2.234(3)	2.4100(10)	2.2085(14)
M(1)−X(1)	2.340(3)	2.5127(9)	2.3400(14)
M(2)−O(1)	1.947(6)	1.975(4)	1.998(3)
M(2)−N(4)	2.072(7)	2.061(5)	2.129(4)
M(2)−N(3)	2.077(7)	2.000(5)	2.115(4)
M(2)−X(3)	2.292(2)	2.4378(10)	2.2544(14)
M(2)−X(1)	2.403(2)	2.4779(9)	2.3920(13)
N(1)−C(13)	1.258(9)	1.285(7)	1.287(6)
N(4)−C(31)	1.293(11)	1.284(7)	1.270(7)
M(1)···M(2)	3.186(5)	3.111(4)	3.209(4)
M(1)−O(1)−M(2)	103.9(2)	102.54(16)	101.63(13)
N(2)−M(1)−O(1)	85.9(2)	88.88(17)	82.55(14)
N(2)−M(1)−N(1)	77.8(3)	80.42(18)	77.36(15)
O(1)−M(1)−N(1)	157.0(2)	166.45(16)	149.90(14)
N(2)−M(1)−X(2)	115.6(2)	114.97(13)	118.74(12)
O(1)−M(1)−X(2)	95.56(17)	89.95(11)	97.70(10)
N(1)−M(1)−X(2)	106.10(19)	102.06(12)	111.53(11)
N(2)−M(1)−X(1)	126.5(2)	136.31(13)	127.22(12)
X(2)−M(1)−X(1)	117.25(9)	107.78(3)	113.19(5)
O(1)−M(2)−N(4)	146.9(3)	156.64(17)	148.00(15)
O(1)−M(2)−N(3)	86.7(3)	90.27(17)	86.56(15)
N(4)−M(2)−N(3)	79.2(3)	81.7(2)	77.09(16)
O(1)−M(2)−X(3)	107.10(16)	99.20(11)	105.21(10)
N(4)−M(2)−X(3)	105.1(2)	103.25(13)	109.37(12)
N(3)−M(2)−X(3)	101.98(19)	94.40(13)	106.12(12)
N(4)−M(2)−X(1)	94.7(2)	95.39(14)	93.48(12)
N(3)−M(2)−X(1)	150.62(19)	158.36(13)	143.92(12)
X(3)−M(2)−X(1)	107.34(9)	107.11(4)	106.70(5)

aryl groups have the effect that one isopropyl substituent per aryl group [C(42), C(7)] lies close to the basal plane of each square pyramid while the other points in a similar direction as a terminal halide [C(39), C(10)]. With regard to the central phenolate plane, one pyridyl-imine unit adopts a pseudo-coplanar conformation [C(25)−C(24)−C(26)−N(3) = 13.5 (**2b**), 16.1 (**2c**), 1.6° (**2d**)], while the other is inclined significantly out-of-this plane [N(2)−C(19)−C(20)−C(25) = 40.8 (**2b**), 28.9 (**2c**), and 36.2° (**2d**)]. As would be expected, the M−X(bridging) distances are longer than the M−X(terminal) distances with some asymmetry apparent between the M−X(bridging) distances [M(1)−X(1) = 2.340(3) (**2b**), 2.5127(9) (**2c**), and 2.3400(14) Å (**2d**) vs M(2)−X(1) = 2.403(2) (**2b**), 2.4779(9) (**2c**), and 2.3920(13) Å (**2d**)]. A similar asymmetry is observed for the M−O(bridging) distances with the M(1)−O(1) bond [2.096(5) (**2b**), 2.012(4) (**2c**), 2.141 Å (**2d**)], in this case, being longer than the M(2)−O(1) bond [1.947(6) (**2b**), 1.975(4) (**2c**), 1.998(3) Å (**2d**)]. The intermetallic M···M distances for all three complexes [Co(1)···Co(2) = 3.186(5) Å (**2b**), Ni(1)···Ni(2) = 3.111(4) Å (**2c**), Zn(1)···Zn(2) 3.209(4) Å (**2d**)] are shorter than those in previously reported complexes containing M(μ-$O_{phenolate}$)(μ-Cl)M [ranges of 3.221−3.235 (M = Co)[18] and 3.221−3.348 Å (M = Zn)[3a,19]] or Ni(μ-$O_{phenolate}$)-(μ-Br)Ni [range of 3.221−3.235 Å[20]] motifs which are reflected by the narrower M−O−M angles [Co(1)−O(1)−Co(2) = 103.9(2)° (**2b**), Ni(1)−O(1)−Ni(2) = 102.54(16)° (**2c**), Zn(1)−O(1)−Zn(2) = 101.63(13)° (**2d**)]. The N(1)−C(1) and N(4)−C(33) bond distances in **2b**−**2d** [∼1.27 Å] are essentially the same as the C=N bond distances in proligand $\mathbf{L^2}$-H [1.281(4) and 1.277(4) Å]. Between structures, the M−N distances (and M−O) follow the order Zn−N > Co−N > Ni−N consistent with the corresponding trend in ionic radii [Zn(II) > $Co(II)_{high\ spin}$ > Ni(II)].

The FAB mass spectra of **2a**−**2d** show fragmentation peaks in each case corresponding to the loss of one or two halide groups from their respective molecular ions. In the IR spectra of **2a**−**2d**, the $\nu(C{=}N)_{imine}$ bands are seen at ∼1587 cm^{-1}; this is indicative of both imino-nitrogen atoms being coordinated to the metal centers. As with **1a**−**1c**, compounds **2a**−**2c** are all paramagnetic with values of the magnetic moments [5.7 (**2a**), 4.7 (**2b**), 3.5 (**2c**) μ_B; Evans Balance at ambient temperature] slightly lower than the corresponding values found for **1a**−**1c**; this is, perhaps, indicative of the onset of some antiferromagnetic behavior at this temperature.[21]

For diamagnetic **2d**, the ^{1}H NMR spectrum (in CD_2Cl_2 at ambient temperature) indicates that the asymmetry observed for the binding sites in the solid state is not maintained in solution as exemplified by the presence of only one type of imino-methyl group (at 2.34 ppm). As with **1d**, restricted rotation of the *N*-aryl groups in **2d** is apparent which is likely further supplemented by inter-aryl steric interactions. Thus, two broad resonances for the CH*Me*$_2$ groups (1.20, 0.98 ppm; in a ratio of 6:18), along with two broad signals both integrating to two protons for the C*H*Me$_2$ protons, are seen at ambient temperature. When the mixture is cooled to −43 °C, however, the broad resonances sharpen to give four separate doublets for the CH*Me*$_2$ groups (0.93, 0.96, 1.00, 1.19 ppm in a ratio of 6:6:6:6) along with two apparent septets for the C*H*Me$_2$ protons; indicative of four separate environments for the methyl groups per *N*-aryl substituent.

In contrast to **2b** and **2d**, crystallization of bromide-containing **2c** from a mixture of acetonitrile−choroform results in the coordination of one molecule of MeCN to give [($\mathbf{L^2}$)$Ni_2Br_3(CH_3CN)$] [**2c**(NCMe)] (Scheme 2). Complex **2c**(NCMe) has been characterized by FAB mass spectrometry along with IR spectroscopy (see Table 2 and Experimental Section). In addition, a crystal of **2c**(NCMe) has been the subject of a single X-ray diffraction study. The molecular structure of **2c**(NCMe) is depicted in Figure 5; selected bond lengths and angles are listed in Table 5.

The molecular structure of **2c**(NCMe) reveals a bimetallic complex similar to that described for **2c**, but it differs in that one molecule of acetonitrile is additionally bound to Ni(2) with the result that the geometry at Ni(2) is distorted octahedral with $N(5)_{NCMe}$ and N(3) disposed mutually trans [N(3)−N(2)−N(5) = 174.7(2)°]. At Ni(1), the square pyramidal [τ = 0.15] geometry is maintained. The effect of

(18) Quijano, E. R.; Stevens, Charles, E. D.; O'Connor, J. *Inorg. Chim. Acta* **1990**, *177*, 267.
(19) You, Z.-L.; Zhu, H.-L. *Z. Anorg. Allg. Chem.* **2006**, *632*, 140.
(20) Adams, H.; Clunas, S.; Fenton, D. E. *Acta Crystallogr.* **2004**, *E60*, m338. (b) Fenton, D. E. *Inorg. Chem. Commun*. **2002**, *5*, 537.
(21) (a) Sakiyama, H.; Ito, R.; Kumagai, H, Inoue, K.; Sakamoto, M.; Nishida, Y.; Yamasaki, M. *Eur. J. Inorg. Chem.* **2001**, 2027. (b) Nanda, K. K.; Das, R.; Thompson, L. K.; Venkastsubramanian, K.; Paul, P.; Nag, K. *Inorg. Chem.* **1994**, *33*, 1188.

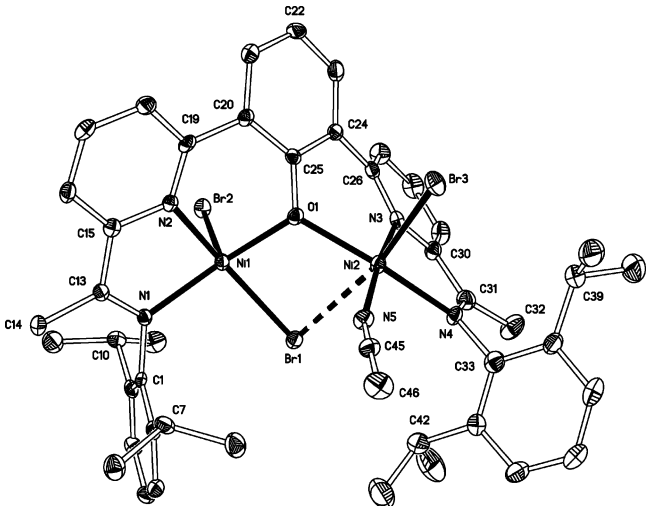

Figure 5. Molecular structure of **2c**(NCMe) with atom labeling scheme and ellipsoids at 30% probability. All hydrogen atoms have been omitted for clarity.

Table 5. Selected Bond Distances (Å) and Angles (deg) for **2c**(NCMe)

Ni(1)−O(1)	1.984(4)	Ni(2)−O(1)	2.056(4)
Ni(1)−N(2)	2.028(4)	Ni(2)−N(3)	1.998(5)
Ni(1)−N(1)	2.079(4)	Ni(2)−N(5)	2.019(5)
Ni(1)−Br(1)	2.4429(10)	Ni(2)−Br(3)	2.4888(11)
Ni(1)−Br(2)	2.4521(10)	Ni(2)−Br(1)	2.8182(11)
N(1)−C(13)	1.283(7)	Ni(2)−N(4)	2.124(5)
Ni(1)···Ni(2)	3.449(4)	N(4)−C(31)	1.282(7)
Ni(1)−O(1)−Ni(2)	117.29(18)	N(3)−Ni(2)−N(5)	174.7(2)
O(1)−Ni(1)−N(2)	85.35(17)	N(3)−Ni(2)−O(1)	86.83(17)
O(1)−Ni(1)−N(1)	150.14(16)	N(5)−Ni(2)−N(4)	95.08(19)
N(2)−Ni(1)−Br(1)	158.98(13)	O(1)−Ni(2)−N(4)	161.36(17)
N(1)−Ni(1)−Br(1)	99.01(13)	N(5)−Ni(2)−Br(1)	86.57(15)
O(1)−Ni(1)−Br(2)	101.16(11)	N(4)−Ni(2)−Br(1)	93.27(14)
N(1)−Ni(1)−Br(2)	105.94(13)	Br(3)−Ni(2)−Br(1)	166.53(4)
Br(1)−Ni(1)−Br(2)	105.85(4)		

acetonitrile coordination is 2-fold. First, the degree of asymmetry present in the Ni−Br(bridging) distances [Ni(1)−Br(1) = 2.4429(10) vs $Ni(2)_{MeCN}$−Br(1) = 2.8182(11) Å] is significantly increased when compared to the corresponding distances in **2c** (Table 4) and to the related dinickel species [(2,6-bis[2-(dimethylamino)-ethyliminomethyl]-4-methylphenolato)$Ni_2(\mu$-Br)$Br(OH_2)_3$]Br.[20a] In fact, the $Ni(2)_{MeCN}$−Br(1) distance could be considered more of an interaction than a bond. Second, the Ni···Ni separation [3.445(4) Å] is considerably longer than that observed in **2c** [3.111(4) Å] and in related Ni(μ-$O_{phenolate}$)(μ-Br)Ni-containing compounds (range of 3.221−3.235 Å)[20] with the corresponding Ni−O−Ni angle [117.29(18)°] more expanded. Furthermore, the flexibility of $(\mathbf{L^2})^-$ is revealed by comparison of **2c**(NCMe) with **2c**, with the central phenolate group in **2c**(NCMe) now tilted away from coplanarity with respect to both adjacent pyridyl-imine planes [N(2)−C(19)−C(20)−C(25) = 24.7°, C(25)−C(24)−C(26)−N(3) = 38.5°].

The FAB mass spectrum for **2c**(NCMe) shows fragmentation peaks similar to that observed for **2c**. In the IR spectra of **2c**(NCMe), the $\nu(C{=}N)_{imine}$ band is seen at 1590 cm^{-1} with an additional band at 2300 cm^{-1} corresponding to the $\nu(C{\equiv}N)$ absorption for the η^1-bound acetonitrile molecule.[22] The paramagnetic properties (μ_{eff} = 3.5 μ_B; Evans balance at room temperature) of **2c**(NCMe) are comparable to that found for **2c**.

The partial displacement of a bridging bromide and reorganization of $(\mathbf{L^2})^-$ upon conversion of **2c** to **2c**(NCMe) was unexpected and notably did not occur on treatment of chloride-bridged **2a**, **2b**, and **2d** with acetonitrile. It might be argued that the metal center possessing the more distorted geometry in **2** [e.g., Co(1) τ = 0.51 (**2b**), Ni(1) τ = 0.50 (**2c**), Zn(1) τ = 0.38 (**2d**)] is more susceptible to the approach of a suitable monodentate ligand which is further aided by the reduction in the inter-aryl steric interactions that would ensue. The explanation as to why this occurs uniquely for **2c** is uncertain, but it could be the result of the relative strengths of a μ-X ligand (X = Br vs Cl).

Screening of Complexes as Catalysts for Ethylene Oligomerization. All the iron, cobalt, and nickel complexes were screened as precatalysts for oligomerization or polymerization of ethylene. Typically, a complex in toluene was treated with 600 equiv (300 equiv/metal center) of methylalumoxane (MAO) at room temperature, and ethylene (1 bar) gas was introduced over a period of 30 min. All the nickel and cobalt systems displayed low activities for ethylene oligomerization affording hydrocarbon-based materials that were readily soluble in chloroform; both iron systems were inactive. No evidence for higher molecular weight polymeric materials could be detected under these experimental conditions. The results of the tests are collected in Table 6 (entries 1−4).

The most active system employed **1c** as the precatalyst (entry 2) affording a film typical of the products obtained with pyridyl-imine-based nickel systems.[14a,14b,23] In the ^{1}H NMR spectrum, very low levels of terminal and internal unsaturation are accompanied by higher levels of methyl chain ends. The ^{13}C NMR spectrum indicates that the oligomeric product contains significant quantities of methyl branches; no evidence for longer-chain branching is apparent. Further inspection of the ^{13}C NMR spectrum reveals the separation between methyl branches to be mainly five or more CH_2 units, while separations of less than one ethylene unit are not present.[24] The activity of **1c**/MAO is comparable with the activity reported for the mononickel analogue [{2-Ph-6-CMe=N(2,6-*i*-$Pr_2C_6H_3$)C_5H_3N}$NiBr_2$]/MAO[25] (under similar conditions), although lower than for the related nonphenyl substituted pyridyl-imine-$NiBr_2$/MAO

(22) Shin, J. H.; Savage, W.; Murphy, V. J.; Bonanno, J. B.; Churchill, D. G.; Parkin, G. *Dalton Trans*. **2001**, 1732.
(23) (a) Laine, T. V.; Lappalainen, K.; Liimatta, J.; Aitola, E.; Lofgren, B.; Leskala, M. *Macromol. Rapid Commun*. **1999**, *20*, 487. (b) Meneghetti, S. P.; Lutz, P. G.; Kress, J. *Organometallics* **1999**, *18*, 2734. (c) Koppl, A.; Alt, H. G. *J. Mol. Catal. A: Chem*. **2000**, *154*, 45. (d) Bres, P. L.; Gibson, V. C.; Mabille, C. D. F.; Reed, W.; Wass, D.; Weatherhead R. H. (BP Chemicals Ltd., U.K.) PCT Int. Appl. WO9849208, 1998; *Chem. Abstr*. **1999**, *130*, 4185.
(24) (a) Usami, T.; Takayama, S. *Macromolecules* **1984**, *17*, 1756. (b) Galland, G. B.; de Souza, R. F.; Mauler, R. S.; Nunes, F. F. *Macromolecules* **1999**, *32*, 1620. (c) Linderman, L. P.; Adams, N. O. *Anal. Chem*. **1971**, *43*, 1245. (d) De Pooter, M.; Smith, P. B.; Dohrer, K. K.; Bennett, K. F.; Meadows, M. D.; Smith, C. G.; Schouwenaars, H. P.; Geerards, R. A. *J. Appl. Polym. Sci*. **1991**, *42*, 399.
(25) Weinberg, W. H.; McFarland, E.; Goldwasser, I.; Boussie, T.; Turner, H.; Van Beek, J. A. M.; Murphy, V.; Powers, T. (Symx Technologies) International Patent WO9803521, 1998.

Table 6. Results of the Catalytic Evaluation of the Cobalt and Nickel Systems[a]

entry	precatalyst	mass[b] (g)	activity (g mmol^{-1} h^{-1} bar^{-1})	external olefin[c] (%)	internal olefin[c] (%)	vinylidenes and trisubstituted[c] (%)	av carbon content[c] (C_n)
1	**1b**	0.010	2	35.9	59.5	5.1	15.7
2	**1c**	0.200	40	59.4	40.6		158.8
3	**2b**	0.050	10	31.7	53.5	14.8	17.5
4	**2c**	0.070	14	58.4	41.6		50.5

[a] General conditions: 1 bar ethylene Schlenk test carried out in toluene (40 mL) at ambient temperature using 6.0 mmol MAO (Al:M = 300:1), 0.01 mmol precatalyst, over 0.5 h. Reactions were terminated by the addition of dilute HCl. [b] Mass of oligomer isolated. [c] Oligomerization product percentages and average carbon content, C_n, calculated via integration of ^{1}H NMR spectra.

systems.[14a,14b,23] The introduction of a bridging phenolate group in **2c** also allows for an active catalytic system (entry 4), in this case, affording a waxy material but exhibiting a lower productivity when compared with that observed for **1c**/MAO. In addition, the average carbon content (C_n) for the oligomer obtained using **2c**/MAO is reduced in comparison with that obtained using **1c**/MAO. The microstructural properties of the oligomer furnished are, however, similar to that produced employing **1c**/MAO with methyl branches predominating.

Both cobalt systems display only low activities (entries 1, 3) with the phenolate-bridged **2b** giving the more active system (entry 3). The ^{1}H NMR spectra of the low molecular weight oligomers obtained indicates in both cases the presence of mixtures of linear α-olefins and internal olefins along with lower degrees of vinylidenes, $R^1R^2C{=}CH_2$ and trisubstituted alkenes $R^1R^2C{=}CHR^3$ (C_6-C_{26}). Unlike with the nickel systems, no evidence for methyl branched structures is evident from the ^{13}C NMR spectra.

For both the nickel and cobalt systems, a coordination−insertion mechanism seems likely, followed by β-hydride elimination (chain transfer). Furthermore, an isomerization process (chain walking) appears operational for both cobalt and nickel. However, only in the case of the nickel systems is the chain walking competitive with the chain propagation with the effect that further insertions of ethylene into a secondary metal−alkyl bond can occur to give the distinctive branched microstructures.[9c] On the other hand, for the cobalt systems, the isomerization process allows for a broader distribution of unsaturated products with small quantities of vinylidenes and trisubstituted compounds also evident. Nevertheless, given the low molecular weight of the materials, it is clear that the ligand frames $\mathbf{L^1}$ and $(\mathbf{L^2})^-$ possess insufficient steric bulk to prevent chain transfer of the growing oligomeric chain.

Conclusions

In this study, we have shown that two new classes of binucleating ligands [$\mathbf{L^1}$, $(\mathbf{L^2})^-$] can be readily accessed in which sterically bulky groups can be introduced at the termini of the ligand manifolds. The coordination chemistry of the resulting complexes has been investigated, and it has been shown that $\mathbf{L^1}$ promotes the formation of remote bis(MX_2) bimetallic units while $(\mathbf{L^2})^-$ favors the formation of $M_2(\mu\text{-}X)X_2$-type complexes in which the metal centers are more closely located. Significantly, all the dicobalt and -nickel systems display some activity for alkene oligomerization upon activation with MAO with the cobalt systems forming mainly a mixture of linear α-olefins and internal olefins while the Ni systems additionally promote methyl branched structures. No pronounced effect with regard to microstructural variations of the oligomeric material is apparent between ligand frames for a given bimetallic center, although variations in productivity are noticeable. The mechanistic role of the two metal centers during oligomerization, however, remains uncertain and indeed the role of cooperative effects is unclear. Nevertheless, the capacity of these sterically bulky compartmental ligands to act as effective scaffolds for two oligomerization-active metal centers has been demonstrated. The role of electronic and steric variation will be probed elsewhere as will the ability of these systems to mediate alternative catalytic transformations.

Experimental Section

All reactions, unless otherwise stated, were carried out under an atmosphere of dry, oxygen-free nitrogen, using standard Schlenk techniques or in a nitrogen purged glovebox. Solvents were distilled under nitrogen from appropriate drying agents and degassed prior to use.[26] The infrared spectra were recorded on a Perkin-Elmer Spectrum One FT-IR spectrometer on solid samples. The ES (electrospray) and FAB (fast atom bombardment) mass spectra were recorded using a micromass Quattra LC mass spectrometer and a Kratos Concept spectrometer with dichloromethane or NBA as the matrix, respectively. High-resolution FAB mass spectra were recorded on Kratos Concept spectrometer (xenon gas, 7 kV) with NBA as matrix. Oligomer products were analyzed by GC, using a Perkin-Elmer Autosystem XL chromatograph equipped with a flame ionization detector, a 30 m PE-5 column (0.25 mm thickness), an injector temperature of 45 °C, and the following temperature program: 45 °C for 7 min, 45−195 °C at 10 °C min^{-1}, 195 °C for 5 min, 195−225 °C at 10 °C min^{-1}, 225 °C for 5 min, 225−250 °C at 10 °C min^{-1}, and 250 °C for 22 min. ^{1}H and ^{13}C NMR spectra were recorded on a Bruker ARX spectrometer (300 MHz) at ambient temperature unless otherwise stated; chemical shifts (ppm) are referred to the residual protic solvent peaks, and chemical shifts are in hertz (Hz). Magnetic susceptibility studies were performed using an Evans balance (Johnson Matthey) at room temperature. The magnetic moment data were calculated following standard methods,[27] and corrections for underlying diamagnetism were applied to data.[28] Elemental analyses were performed at the Science Technical Support Unit, London Metropolitan University.

The reagents, 1,3-dibromobenzene, 2,6-dibromophenol, 2,6-diisopropylaniline, (DME)$NiBr_2$ (DME = 1,2-dimethoxyethane),

(26) Armarego W. L. F.; Perrin, D. D. In *Purification of Laboratory Chemicals*, 4th ed.; Butterworth Heinemann: Woburn, MA, 1996.
(27) Mabbs, F. E.; Machin, D. J. *Magnetism and Transition Metal Complexes*; Chapman and Hall: London, 1973.
(28) (a) O'Connor, C. J. *Prog. Inorg. Chem.* **1982**, *29*, 203. (b) *Handbook of Chemistry and Physics*, 70th ed.; Weast, R. C., Ed.; CRC Press: Boca Raton, FL, 1990; p E134.

MAO (10 wt % in toluene), cuprous bromide, and the metal dichlorides were purchased from Aldrich Chemical Co. and were used without further purification. The compounds tetrakis(triphenylphosphine)palladium(0)[29] and 6-tributylstannyl-2-(2-methyl-1,3-dioxolan-2-yl)pyridine[10] were prepared according to previously reported procedures. All other chemicals were obtained commercially and used without further purification.

Synthesis of 2,6-{(O═C(Me)C_5H_3N}$_2C_6H_4$. 1,3-Dibromobenzene (0.472 g, 2.00 mmol), 6-tributylstannyl-2-(2-methyl-1,3-dioxolan-2-yl)pyridine (2.00 g, 4.40 mmol, 2.2 equiv), and tetrakis-(triphenylphosphine)palladium(0) (0.185 g, 0.16 mmol, 0.08 equiv) were loaded in a Schlenk vessel under an atmosphere of nitrogen, and the contents were stirred in dry toluene (25 mL) for 72 h at 90 °C. After removal of the solvent under reduced pressure, the reaction mixture was stirred overnight at 60 °C in 4 M HCl (20 mL), cooled to room temperature, and carefully neutralized by the addition of 4 M $NaHCO_3$. The suspension was extracted with $CHCl_3$ (3 × 30 mL), and the organic phase was separated, washed with water (3 × 30 mL) and brine (1 × 40 mL), and dried over magnesium sulfate. after filtration, the solvent was removed under reduced pressure, and the crude product was crystallized from ethanol at −30 °C. The resulting precipitate was collected by filtration to afford 2,6-{(O═C(Me)C_5H_3N}$_2C_6H_4$ as a white solid. Yield: 60% (0.379 g, 1.20 mmol). ^{1}H NMR (300 MHz, $CDCl_3$): δ 2.87 (s, 6H, C*H*$_3$), 7.67 (t, $^3J_{HH}$ = 7.6, $^3J_{HH}$ = 7.6, 1H, Ar-*H*), 7.95 (app t, $^3J_{HH}$ = 7.6, $^3J_{HH}$ = 7.6, 2H, Py-*H*), 8.0−8.1 (m, 4H, Py-*H* and Ar-*H*), 8.19 (dd, $^3J_{HH}$ = 7.9, $^4J_{HH}$ = 1.7, 2H, Py-*H*), 8.92 (t, $^4J_{HH}$ = 1.7, $^4J_{HH}$ = 1.7, 1H, Ar-*H*). ^{13}C {^{1}H} NMR (75 MHz, $CDCl_3$): δ 25.8 (CH_3), 120.1 (Ar or Py), 123.6 (Ar or Py), 125.6 (Ar), 127.8 (Py), 129.5 (Ar), 137.9 (Py), 139.1 (Ar), 153.5 (Py), 156.1 (Py), 200.5 (C═O). IR (cm^{-1}): 2960 (w), 1699 (C═O), 1580 (s), 1443 (m), 1347 (m), 1299 (m), 1235 (m), 1111 (m), 1088 (m), 993 (w), 951 (w), 818 (s), 785 (s), 731 (m). FAB positive mass spectrum (*m*/*z*): 317 [M + H]$^+$. Acc. Mass FAB-MS positive (*m*/*z*) required for ($C_{20}H_{16}N_2O_2H^+$): 317.12900. Found: 317.12894. mp: 147−149 °C.

Synthesis of 2,6-{(O═C(Me)C_5H_3N}$_2C_6H_3$(OH). 2,6-Dibromophenol (3.00 g, 11.90 mmol), 6-tributylstannyl-2-(2-methyl-1,3-dioxolan-2-yl)pyridine (11.84 g, 26.19 mmol, 2.2 equiv), tetrakis-(triphenylphosphine)palladium(0) (1.10 g, 0.95 mmol, 0.08 equiv), and cuprous bromide (0.27 g, 1.90 mmol, 0.16 equiv) were loaded in a Schlenk vessel under an atmosphere of nitrogen, and the contents were stirred in dry toluene (80 mL) for 72 h at 100 °C. After removal of the solvent under reduced pressure, the resulting oil was stirred overnight at 60 °C in 4 M HCl (50 mL), cooled to room temperature, and carefully neutralized by addition of 4 M $NaHCO_3$. The suspension was extracted with $CHCl_3$ (3 × 40 mL), and the organic phase was separated, washed with water (3 × 40 mL), a saturated solution of the disodium salt of EDTA (2 × 30 mL), and brine (1 × 50 mL) and dried over magnesium sulfate. Following filtration, the solvent was removed under reduced pressure, and the crude product was crystallized from ethanol at −30 °C. The resulting precipitate was collected by filtration to afford 2,6-{(O═C(Me)C_5H_3N}$_2C_6H_3$(OH) as a yellow solid. Yield: 57% (2.24 g, 6.78 mmol). ^{1}H NMR (300 MHz, $CDCl_3$): δ 2.81 (s, 6H, C*H*$_3$), 7.14 (t, $^3J_{HH}$ = 7.9, $^3J_{HH}$ = 7.9, 1H, phenol-*H*), 7.9−8.1 (m, 6H, Py-*H* and phenol-*H*), 8.25 (dd, $^3J_{HH}$ = 7.3, $^4J_{HH}$ = 2.3, 2H, Py-*H*). ^{13}C {^{1}H} NMR (75 MHz, $CDCl_3$): δ 26.2 (s, CH_3), 119.4 (s, Py), 119.9 (s, Py), 126.1 (s, phenol), 130.9 (s, phenol), 137.9 (s, Py), 151.5 (s, phenol), 156.0 (s, Py), 157.9 (s, Py), 199.1 (s, C═O). IR (cm^{-1}): 1698 (s, ν(C═O)), 1583 (m), 1452 (m), 1353 (m), 1259 (m), 1138 (w), 1106 (m), 1087 (m), 1004 (m), 950 (w), 853 (w), 823 (m), 784 (s), 737 (s). FAB positive mass spectrum (*m*/*z*): 333 [M + H]$^+$. Acc. Mass FABMS positive spectrum (*m*/*z*) required for ($C_{20}H_{16}N_2O_3H^+$): 333.12394. Found: 333.12392. mp: 178−180 °C.

Synthesis of L^1. 2,6-{(O═C(Me)C_5H_3N}$_2C_6H_4$ (0.853 g, 2.70 mmol) was suspended in 2,6-diisopropylaniline (4.78 g, 27.0 mmol, 10 equiv) and stirred for 15 min at 160 °C on a heating mantle until dissolution. A catalytic amount of formic acid was added, and the reaction mixture was stirred for an additional 20 min at this temperature. After the removal of the excess 2,6-diisopropylaniline under reduced pressure, the resulting brown residue was stirred in ethanol at room temperature, and the resultant precipitate filtered and washed with ethanol. The product was recrystallized from a dichloromethane−hexane (1:9) mixture at room temperature to afford **L^1** as a yellow solid. Yield: 50% (0.857 g, 1.35 mmol). ^{1}H NMR (300 MHz, $CDCl_3$): δ 1.07 (d, $^3J_{HH}$ = 6.7, 12H, CH(C*H*$_3$)$_2$), 1.09 (d, $^3J_{HH}$ = 6.7, 12H, CH(C*H*$_3$)$_2$), 2.26 (s, 6H, C*H*$_3$C═N), 2.71 (sept, $^3J_{HH}$ = 6.7, 4H, C*H*(CH$_3$)$_2$), 7.0−7.1 (m, 6H, Ar$_{N-aryl}$-*H*), 7.56 (dd, $^3J_{HH}$ = 7.9, $^3J_{HH}$ = 7.6, 1H, Ar-*H*), 7.9−7.8 (m, 4H, Py-*H* and Ar-*H*), 8.19 (dd, $^3J_{HH}$ = 7.8, $^4J_{HH}$ = 1.8, 2H, Py-*H*), 8.35 (dd, $^3J_{HH}$ = 7.3, $^4J_{HH}$ = 1.5, 2H, Py-*H*), 9.01 (s, 1H, Ar-*H*). ^{13}C {^{1}H} NMR (75 MHz, $CDCl_3$): δ 17.3 (*C*H$_3$C═N), 22.9 (CH_3), 23.2 (CH_3), 28.3 (CH), 119.8 (Py), 121.2 (Ar), 123.0 (Ar), 123.6 (Py), 125.6 (Ar), 127.5 (Ar), 129.3 (Ar), 135.8 (Py), 137.3 (Ar), 139.6 (Ar), 146.5 (Ar), 155.7 (Py), 156.2 (Py), 167.3 (C═N). IR (cm^{-1}): 2960 (m), 1641 (br, ν(C═N)$_{imine}$), 1572 (m), 1448 (m), 1381 (m), 1360 (m), 1307 (m), 1235 (m), 1119 (m), 1092 (s), 817 (m), 786 (s), 765 (s), 689 (s). ES positive mass spectrum (*m*/*z*): 635 [M + H]$^+$. Acc. Mass FABMS positive (*m*/*z*) required for ($C_{44}H_{50}N_4H^+$): 635.41137. Found: 635.41138. mp: 204−206 °C.

Synthesis of L^2-H. A similar procedure to that outlined for **L^1** was employed using 2,6-{(O═C(Me)C_5H_3N}$_2C_6H_3$(OH) (0.896 g, 2.70 mmol) in 2,6-diisopropylaniline (4.78 g, 27.0 mmol, 10 equiv). After the removal of the excess 2,6-diisopropylaniline under reduced pressure, the resulting brown residue was stirred in ethanol at room temperature, and the resultant precipitate was filtered and washed with ethanol to afford **L^2**-H as a yellow solid. Yield: 50% (0.878 g, 1.35 mmol). Crystals suitable for the X-ray determination were grown by slow evaporation of a chloroform solution containing **L^2**-H. Anal. Calcd for ($C_{44}H_{50}N_4O\cdot 3H_2O$): C, 75.00; H, 7.95; N, 7.95%. Found: C, 74.83; H, 8.04; N, 8.04%. ^{1}H NMR (300 MHz, $CDCl_3$): δ 1.16 (d, $^3J_{HH}$ = 6.8, 12H, CH(C*H*$_3$)$_2$), 1.17 (d, $^3J_{HH}$ = 6.8, 12H, CH(C*H*$_3$)$_2$), 2.30 (s, 6H, C*H*$_3$C═N), 2.76 (sept, $^3J_{HH}$ = 6.8, 4H, C*H*(CH$_3$)$_2$), 7.0−7.2 (m, 7H, Ar-*H* and phenol-*H*), 7.96 (app. t, $^3J_{HH}$ = 7.9, $^3J_{HH}$ = 7.9, 2H, Py-*H*), 8.05 (d, $^3J_{HH}$ = 7.9, 2H, phenol-*H*), 8.22 (d, $^3J_{HH}$ = 7.9, 2H, Py-*H*), 8.33 (d, $^3J_{HH}$ = 7.9, 2H, Py-*H*). ^{13}C{^{1}H} NMR (75 MHz, $CDCl_3$): δ 16.4 (s, *C*H$_3$C═N), 21.9 (s, CH_3), 22.2 (s, CH_3), 27.3 (s, CH), 118.1 (s, Py), 118.4 (s, Py), 122.0 (s, Ar), 122.6 (s, Ar), 123.1 (s, phenol), 129.4 (s, phenol), 134.7 (s, Py), 136.4 (s, phenol), 145.3 (s, Ar), 153.4 (s, phenol), 154.6 (s, Py), 156.9 (s, Py), 165.0 (s, C═N). IR (cm^{-1}): 2958 (m), 1637 (m, ν(C═N)), 1590 (m), 1566 (m), 1438 (m), 1361 (m), 1263 (m), 1110 (m), 1041 (w), 796 (w), 784 (s), 760 (s) and 743 (s). ES positive mass spectrum (*m*/*z*): 651 [M + H]$^+$. Acc. Mass FABMS positive spectrum (*m*/*z*) required for ($C_{44}H_{50}N_4OH^+$): 651.40630. Found: 651.40629. mp: 266−268 °C.

Synthesis of [(L^1)M$_2$X$_4$] (1). (a) 1a (M = Fe, X = Cl). An oven-dried Schlenk flask equipped with a magnetic stir bar was evacuated and backfilled with nitrogen. The flask was charged with anhydrous $FeCl_2$ (0.040 g, 0.315 mmol) in *n*-BuOH (10 mL), and the contents were stirred at 110 °C until the iron salt had completely dissolved.

(29) Tellier, F.; Sauvetre, R.; Normant, J.-F. *J. Organomet. Chem.* **1985**, *292*, 2.

Table 7. Crystallographic and Data Processing Parameters for $\mathbf{L^2}$-H, **1c**, **2b**, **2c**, **2c**(NCMe), and **2d**[a]

	$\mathbf{L^2}$-H	**1c**	**2b**
formula	$C_{44}H_{50}N_4O$	$C_{44}H_{50}Br_4N_4Ni_2 \cdot 1.5CH_3CN$	$C_{44}H_{49}Cl_3N_4OCo_2 \cdot CH_3CN$
M	650.88	1133.52	915.14
cryst size (mm^3)	0.23 × 0.20 × 0.12	0.28 × 0.20 × 0.10	0.38 × 0.29 × 0.08
temp (k)	150(2)	150(2)	150(2)
cryst syst	triclinic	monoclinic	triclinic
space group	$P\bar{1}$	$C2/c$	$P\bar{1}$
a (Å)	9.2269(15)	43.915(7)	12.549(5)
b (Å)	12.510(2)	8.3993(14)	13.765(6)
c (Å)	16.952(3)	26.110(4)	14.456(6)
α (deg)	83.535(3)	90	80.417(7)
β (deg)	82.322(4)	90.700(3)	77.167(6)
γ (deg)	70.485(3)	90	74.026(7)
U ($Å^3$)	1823.0(5)	9630(3)	2325.8(16)
Z	2	8	2
D_c (Mg m^{-3})	1.186	1.564	1.307
F(000)	700	4568	952
μ(Mo Kα) (mm^{-1})	0.071	4.139	0.924
reflns collected	13 346	36 368	16 645
independent reflns	6357	9476	8111
R_{int}	0.0809	0.0811	0.2085
restraints/params	0/452	0/517	0/519
final R indices	R1 = 0.0724	R1 = 0.0508	R1 = 0.0828,
($I > 2\sigma(I)$)	wR2 = 0.1277	wR2 = 0.0854	wR2 = 0.1821
all data	R1 = 0.1516	R1 = 0.0965	R1 = 0.1813
	wR2 = 0.1531	wR2 = 0.0957	wR2 = 0.2196
GOF on F^2 (all data)	0.936	0.897	0.912

	2c	**2c**(NCMe)	**2d**
formula	$C_{44}H_{49}Br_3N_4ONi_2 \cdot CHCl_3$	$C_{46}H_{52}Br_3N_5ONi_2 \cdot 3CH_3CN \cdot 0.5H_2O$	$C_{44}H_{49}Cl_3N_4OZn_2 \cdot CH_3CN$
M	1126.3	1180.25	928.02
cryst size (mm^3)	0.22 × 0.16 × 0.07	0.33 × 0.24 × 0.18	0.38 × 0.36 × 0.15
temp (k)	150(2)	150(2)	150(2)
cryst syst	monoclinic	triclinic	triclinic
space group	$P2_1/c$	$P\bar{1}$	$P\bar{1}$
a (Å)	13.6891(19)	13.267(3)	12.1071(19)
b (Å)	34.633(5)	14.100(3)	13.864(2)
c (Å)	10.2467(14)	16.802(4)	14.704(2)
α (deg)	90	65.587(4)	80.680(3)
β (deg)	107.021(3)	78.435(4)	76.300(3)
γ (deg)	90	66.968(4)	75.191(2)
U ($Å^3$)	4645.1(11)	2631.1(11)	2304.8(6)
Z	4	2	2
D_c (Mg m^{-3})	1.611	1.490	1.337
F(000)	2272	1206	964
μ(Mo Kα) (mm^{-1})	3.602	3.039	1.254
reflns collected	33 459	20 612	16 837
independent reflns	8165	10 213	8062
R_{int}	0.0858	0.0519	0.0446
restraints/params	0/533	0/ 618	0/543
final R indices	R1 = 0.0525,	R1 = 0.0465	R1 = 0.0586
($I > 2\sigma(I)$)	wR2 = 0.0996	wR2 = 0.0916	wR2 = 0.1512
all data	R1 = 0.0913	R1 = 0.0847	R1 = 0.0824
	wR2 = 0.0996	wR2 = 0.0992	wR2 = 0.1636
GOF on F^2	0.943	0.890	1.048

[a] Data in common: graphite-monochromated Mo Kα radiation, $\lambda = 0.71073$ Å; $R1 = \sum||F_o| - |F_c||/\sum|F_o|$, $wR2 = [\sum w(F_o^2 - F_c^2)^2/\sum w(F_o^2)^2]^{1/2}$, $w^{-1} = [\sigma^2(F_o)^2 + (aP)^2]$, $P = [\max(F_o^2,0) + 2(F_c^2)]/3$, where a is a constant adjusted by the program; $GOF = [\sum(F_o^2 - F_c^2)2/(n - p)]^{1/2}$, where n is the number of reflections and p the number of parameters.

$\mathbf{L^1}$ (0.100 g, 0.158 mmol, 0.5 equiv) was added, and the reaction mixture was stirred at 110 °C for a further 20 min. After it was cooled to room temperature, the suspension was concentrated, and hexane was added to induce precipitation of the product. The solid was filtered, washed with hexane, and dried overnight under reduced pressure to afford [($\mathbf{L^1}$)Fe_2Cl_4] (**1a**) as a brown powder. Yield: 68% (0.095 g, 0.107 mmol). IR (cm^{-1}): 2965 (w), 1626 (w), 1593 (m, ν(C═N)$_{imine}$), 1575 (m), 1455 (m), 1443 (m), 1376 (m), 1321 (w), 1276 (w), 1251 (m), 1190 (m), 1025 (m), 933 (w), 818 (w), 800 (s), 791 (s), 775 (s), 711 (s).

(b) 1b (M = Co, X = Cl). A procedure analogous to that described for **1a**, employing $CoCl_2$ (0.041 g, 0.315 mmol) and $\mathbf{L^1}$ (0.100 g, 0.158 mmol, 0.5 equiv), gave [($\mathbf{L^1}$)Co_2Cl_4] (**1b**) as a blue powder. Yield: 45% (0.063 g, 0.071 mmol). IR (cm^{-1}): 2961 (w), 1622 (w), 1593 (m, ν(C═N)$_{imine}$), 1565 (w), 1456 (m), 1442 (m), 1386 (w), 1370 (w), 1317 (w), 1255 (m), 1194 (w), 1014 (m), 935 (w), 827 (w), 803 (s), 794 (s), 777 (s), 710 (s).

(c) 1c (M = Ni, X = Br). A procedure analogous to that described for **1a**, employing $NiBr_2$ (0.097 g, 0.315 mmol) and $\mathbf{L^1}$ (0.100 g, 0.158 mmol, 0.5 equiv), gave [($\mathbf{L^1}$)Ni_2Br_4] (**1c**) as a red powder. Yield: 72% (0.101 g, 0.087 mmol). Red crystals suitable for X-ray analysis were grown by slow cooling of a hot acetonitrile solution containing **1c**. IR (cm^{-1}): 2963 (m), 1620 (w), 1594 (m, ν(C═N)$_{imine}$), 1569 (w), 1456 (m), 1441 (m) 1386 (w), 1371 (w),

1321 (m), 1254 (m), 1193 (w), 1017 (m), 933 (w), 823 (w), 804 (s), 792 (s), 778 (s), 709 (s).

(d) 1d (M = Zn, X = Cl). A procedure analogous to that described for **1a**, employing $ZnCl_2$ (0.043 g, 0.315 mmol) and **L**[1] (0.100 g, 0.158 mmol, 0.5 equiv), gave [(**L**[1])Zn_2Cl_4] (**1d**) as a yellow powder. Yield: 55% (0.093 g, 0.087 mmol). ^{1}H NMR (300 MHz, $CDCl_3$): δ 1.01 (d, 12H, $^3J_{HH}$ = 6.7, CH(CH_3)$_2$), 1.25 (d, 12H, $^3J_{HH}$ = 6.7, CH(CH_3)$_2$), 2.40 (s, 6H, CH_3C═N), 2.88 (sept, 4H, $^3J_{HH}$ = 6.7, CH(CH$_3$)$_2$), 7.1−7.3 (m, 6H, Ar-*H*), 7.82 (dd, 1H, $^3J_{HH}$ = 7.6, $^3J_{HH}$ = 7.9, Ar-*H*), 8.0−8.1 (m, 4H, Ar-*H* and Py-*H*), 8.25 (dd, 2H, $^3J_{HH}$ = 7.6, $^3J_{HH}$ = 7.9, Py-*H*), 8.42 (d, 2H, $^3J_{HH}$ = 7.9, Py-*H*), 8.68 (s, 1H, Ar-*H*). IR (cm^{-1}): 2963 (w), 1632 (w), 1592 (m, ν(C═N)$_{imine}$), 1562 (w), 1455 (m), 1442 (m) 1385 (w), 1370 (m), 1312 (w), 1254 (s), 1196 (m), 1014 (w), 933 (w), 849 (w), 823 (w), 805 (s), 795 (s), 777 (s), 712 (s).

Synthesis of [(L[2])M$_2$(μ-X)X$_2$] (2). (a) 2a (M = Fe, X = Cl). An oven-dried Schlenk flask equipped with a magnetic stir bar was evacuated and backfilled with nitrogen. The flask was charged with anhydrous $FeCl_2$ (0.039 g, 0.308 mmol) in *n*-BuOH (10 mL), and the contents were heated to 110 °C until the iron salt had completely dissolved. **L**[2]-H (0.100 g, 0.154 mmol, 0.5 equiv) was added, and the mixture was heated to 110 °C for a further 20 min. After it was cooled to room temperature, the suspension was concentrated and washed several times with hexane. The solid was dried overnight under reduced pressure to afford [(**L**[2])Fe_2(μ-Cl)Cl_2] (**2a**) as a brown dark solid. Yield: 55% (0.093 g, 0.087 mmol). IR (cm^{-1}): 2964 (m), 1616 (w), 1588 (s, ν(C═N)$_{imine}$), 1552 (m), 1446 (s), 1366 (m), 1322 (m), 1251 (m), 1194 (m), 1104 (w), 1006 (w), 822 (m), 791 (s), 773 (s), 753 (m).

(b) 2b (M = Co, X = Cl). A procedure analogous to that described for **2a,** employing $CoCl_2$ (0.040 g, 0.308 mmol) and **L**[2]-H (0.100 g, 0.154 mmol, 0.5 equiv), gave [(**L**[2])Co_2(μ-Cl)Cl_2] **2b** as a blue-green solid. Yield: 35% (0.054 g, 0.052 mmol). Blue crystals suitable for X-ray analysis were grown by slow cooling of a hot acetonitrile solution containing **2b**. IR (cm^{-1}): 2964 (w), 1620 (w), 1586 (s, ν(C═N)$_{imine}$), 1551 (m), 1476 (w), 1442 (s), 1408 (m), 1365 (m), 1288 (w), 1252 (m), 1191 (m), 1112 (m), 1060 (m), 1011 (m), 854 (m), 826 (m), 790 (s), 757 (s), 738 (m).

(c) 2c (M = Ni, X = Br). A procedure analogous to that described in **2a**, employing (DME)$NiBr_2$ (0.094 g, 0.308 mmol) and **L**[2]-H (0.100 g, 0.154 mmol, 0.5 equiv), gave [(**L**[2])Ni_2(μ-Br)-Br_2] (**2c**) as an orange solid. Yield: 55% (0.092 g, 0.085 mmol). Red crystals suitable for X-ray analysis were grown by layering of a chloroform solution of the complex with diethyl ether. IR (cm^{-1}): 2963 (w), 1620 (w), 1589 (s, ν(C═N)$_{imine}$), 1552 (m), 1446 (s), 1417 (m), 1387 (w), 1366 (m), 1324 (w), 1276 (m), 1241 (m), 1195 (m), 1103 (w), 1060 (w), 1021 (m), 858 (m), 823 (m), 784 (s), 774 (s), 740 (s).

(d) 2d (M = Zn, X = Cl). A procedure analogous to that described in **2a**, employing $ZnCl_2$ (0.042 g, 0.308 mmol) and **L**[2]-H (0.100 g, 0.154 mmol, 0.5 equiv), gave [(**L**[2])Zn_2(μ-Cl)Cl_2] (**2d**) as a yellow solid. Yield: 50% (0.068 g, 0.077 mmol). Yellow crystals suitable for X-ray analysis were grown by slow cooling of a hot acetonitrile−chloroform solution containing **2d**. ^{1}H NMR (300 MHz, CD_2Cl_2, 300 K): δ 0.98 (br, 18H, CH(CH_3)$_2$), 1.20 (br, 6H, CH(CH_3)$_2$), 2.34 (s, 6H, CH_3C═N), 2.87 (br, 2H, CH(CH$_3$)$_2$), 3.05 (br, 2H, CH(CH$_3$)$_2$), 6.87 (tr, $^3J_{HH}$ = 8.2, $^3J_{HH}$ = 8.2, 1H, phenolate-*H*), 7.1−7.3 (m, 6H, Ar-*H*), 7.76 (d, $^3J_{HH}$ = 7.8, 2H, phenolate-*H*), 7.92 (dd, $^3J_{HH}$ = 7.0, $^4J_{HH}$ = 1.9, 2H, Py-*H*), 7.9−8.1 (m, 4H, Py-*H*). ^{1}H NMR (300 MHz, CD_2Cl_2, 230 K): δ 0.93 (d, $^3J_{HH}$ = 6.7, 6H, CH(CH_3)$_2$), 0.96 (d, $^3J_{HH}$ = 6.7, 6H, CH(CH_3)$_2$), 1.00 (d, $^3J_{HH}$ = 6.7, 6H, CH(CH_3)$_2$), 1.19 (d, $^3J_{HH}$ = 6.7, 6H, CH(CH_3)$_2$), 2.37 (s, 6H, CH_3C═N), 2.77 (app. sept, $^3J_{HH}$ = 6.7, 2H, CH(CH$_3$)$_2$), 3.04 (app. sept, $^3J_{HH}$ = 6.7, 2H CH(CH$_3$)$_2$), 7.03 (tr, $^3J_{HH}$ = 7.8, $^3J_{HH}$ = 7.8, 1H, phenolate-*H*), 7.2−7.3 (m, 6H, Ar-*H*), 7.89 (d, $^3J_{HH}$ = 7.8, 2H, phenolate-*H*), 7.89 (d, $^3J_{HH}$ = 7.4, 2H, Py-*H*), 8.17 (d, $^3J_{HH}$ = 7.4, 2H, Py-*H*), 8.23 (d, $^3J_{HH}$ = 7.8, 2H, Py-*H*). IR (cm^{-1}): 2964 (w), 1628 (m), 1588 (s, ν(C═N)$_{imine}$), 1552 (m), 1448 (s), 1366 (m), 1321 (m), 1254 (m), 1191 (m), 1010 (m), 826 (s), 790 (s), 772 (s), 748 (s).

Synthesis of [(L[2])Ni$_2$Br$_3$(NCMe)] [2c(NCMe)]. Complex **2c** (0.030 g, 0.030 mmol) was heated to reflux in acetonitrile (1.5 mL) until the complex had partially dissolved. The mixture was filtered through Celite, and the resulting solution was treated with a few drops of $CHCl_3$ and then left to stand at room temperature for 1 day to give [(**L**[2])Ni_2Br_3(NCMe)] [**2c**(NCMe)] as dark red crystals. The spectroscopic and spectrometric data were similar to those for **2c** (see Table 2).

Screening for Ethylene Oligomerization. An oven-dried 200 mL Schlenk vessel equipped with magnetic stir bar was evacuated and backfilled with nitrogen. The vessel was charged with the precatalyst (0.01 mmol) dissolved in toluene (40 mL), and MAO was introduced (6.0 mmol, 300 equiv/metal center). After a period of 5 min, the vessel was purged with ethylene, and the contents were magnetically stirred under 1 bar of ethylene pressure at room temperature for the duration of the test. After 0.5 h, the test was terminated by the addition of dilute aqueous hydrogen chloride (5 mL). The organic phase was separated, dried over magnesium sulfate, and analyzed by GC. For analysis of the oligomers by NMR (^{1}H and ^{13}C) spectroscopy, the solvent was removed on the rotary evaporator, and the residue was dissolved in $CDCl_3$.

Crystallographic Studies. Data collection for **L**[2]-H, **1c**, **2b**, **2c**, **2c**(NCMe), and **2d** was carried out on a Bruker APEX 2000 CCD diffractometer using graphite-monochromated Mo Kα radiation (λ = 0.71073 Å). Details of the data collection, refinement, and crystal data are listed in Table 7. The data were corrected for Lorentz and polarization effects, and empirical absorption corrections were applied. Structure solution by direct methods and structure refinement on F^2 were performed with SHELXTL, version 6.10.[30] Hydrogen atoms were included in calculated positions (C−H = 0.96 Å) riding on the bonded atom with isotropic displacement parameters set to 1.5 U_{eq}(C) for methyl H atoms and 1.2 U_{eq}(C) for all other H atoms. Apart from C40 and C41 (atoms were disordered and split) in **2b**, all non-H atoms were refined with anisotropic displacement parameters. Graphical representations of the molecular structures were generated with the program ORTEP.[31]

Acknowledgment. We thank the University of Leicester for financial assistance and Johnson Matthey PLC for the palladium chloride.

Supporting Information Available: CIF files containing all crystallographic data for **L**[2]-H, **1c**, **2b**, **2c**, **2c**(NCMe), and **2d**. This material is available free of charge via the Internet at http://pubs.acs.org. The CIF files have also been deposited at the Cambridge Crystallographic Data Centre with reference numbers 614439−614444. Copies of the data can be obtained free of charge on application to the CCDC, 12 Union Road, Cambridge CB21EZ, U.K. (fax +44 1223 336033; e-mail deposit@ccdc.cam.ac.uk).

IC061286X

(30) Sheldrick, G. M. *SHELXTL*, version 6.10; Bruker AXS, Inc.: Madison, WI, 2000.
(31) *ORTEP 3 for Windows*, version 1.074; Farrugia, L. J. *J. Appl. Crystallogr.* **1997**, *30*, 565.